Acta Metallurgica Sinica (English Letters)
https://doi.org/10.1007/s40195-022-01450-2

Effect of Nanometer WC Coating on Thermal Conductivity of Diamond/6061 Composites

Z. Y. Dong[1,2] · D. Wang[1] · W. G. Wang[3] · B. L. Xiao[1] · Z. Y. Ma[1]

Received: 6 May 2022 / Revised: 10 June 2022 / Accepted: 17 June 2022

Abstract
Diamond has poor interface tolerance with Al. To enhance interface bonding, in this study, tungsten carbide (WC) nanocoatings on the surface of diamond particles were prepared using sol–gel and in-situ reaction methods. WO_3 sol–gel with two concentrations, 0.2 mol/L, and 0.5 mol/L, was, respectively, coated on diamond particles, then sintered at 1250 °C for 2 h to produce WC nanocoatings. The concentration of 0.2 mol/L WO_3 sol–gel was not enough to cover the surface of the diamond completely, while 0.5 mol/L WO_3 sol–gel could fully cover it. Moreover, WO_3 was preferentially deposited on {100} planes of the diamond. WO_3 converted to WC in-situ nanocoatings after sintering due to the in-situ reaction of WO_3 and diamond. The diamond-reinforced Al composites with and without WC coating were fabricated by powder metallurgy. The diamond/Al composite without coating has a thermal conductivity of 584.7 W/mK, while the composite with a coating formed by 0.2 mol/L and 0.5 mol/L WO_3 sol–gel showed thermal conductivities of 626.1 W/mK and 584.2 W/mK, respectively. The moderate thickness of nanocoatings formed by 0.2 mol/L WO_3 sol–gel could enhance interface bonding, therefore improving thermal conductivity. The nanocoating produced by 0.5 mol/L WO_3 sol–gel cracked during the fabrication of the composite, leading to $Al_{12}W$ formation and a decrease in thermal conductivity.

Keywords Diamond · Al matrix composite · Nanometer coating · WC · Thermal conductivity

1 Introduction

With the rapid development of electronic components toward miniaturization and integration, effective heat dissipation is becoming a crucial issue for the safety and reliability of electronic components [1–3]. Therefore, thermal management materials are confronted with imperative demands for improving thermal conductivity (TC). Metal matrix composites (MMCs) with favorable thermal properties and low coefficient of thermal expansion (CTE) are widely used as thermal management materials [4]. However, traditional MMCs, such as Mo/Cu [2], W/Cu [4], SiC/Al [5, 6] have conductivity lower than 200 W/mK which is not high enough to sustain reliable use. Diamond has an extremely high TC as high as 2200 W/mK [7, 8], naturally, diamond-reinforced Al matrix composites have been considered to be ideal thermal management material.

Unfortunately, there exists a big gap between the expected TC and the actual value of diamond/Al composites. Poor wettability between diamond and Al tends to produce defects during the fabrication of the composites, such as cracks and holes, leading to increasing interfacial thermal resistance. Moreover, the large difference in the phonon velocity between diamond and Al also decreases the TC of the diamond/Al composites. To improve the TC of the diamond/Al composites, many attempts have been conducted to enhance the interfacial bonding and bridge the gap of the phonon velocity between diamond and Al alloy, including producing in-situ reaction [9, 10], alloying of Al matrix [11, 12], and introducing coating on the diamond surface [1, 13–18].

Zhang et al. [9] found that generation of Al_4C_3 at the interface of 68 vol.% diamond/Al composites enhanced TC

Available online at http://link.springer.com/journal/40195.

✉ D. Wang
dongwang@imr.ac.cn

1 Shi-changxu Innovation Center for Advanced Materials, Institute of Metal Research, Chinese Academy of Sciences, Shenyang 110016, China

2 School of Materials Science and Engineering, University of Science and Technology of China, Shenyang 110016, China

3 Liaoning Shihua University, Fushun 113001, China

Published online: 23 August 2022

from 655 to 760 W/mK. However, Al_4C_3 decomposes easily in a humid environment, which seriously damages the performance and stability of the composites. Yang et al. [10] reported that the TC of a 62 vol.% diamond/Al composite decreased from 394 to 326 W/mK after being immersed in deionized water for 48 h due to the degradation of Al_4C_3.

Adding carbide-forming elements into the Al matrix has been an important method to improve interfacial bonding. Guo et al. [11] added Si into a pure Al matrix and produced SiC on the interface, which enhanced interfacial bonding. The TC of the composite was slightly increased from 500 to 540 W/mK. However, the additions significantly decrease the TC of the matrix alloy. It has been reported that the addition of 3 wt% of element Si to pure Al matrix resulted in a decrease in TC from 235 to 217 W/mK [12].

Compared to alloying of Al matrix, the surface modification of diamond particles by plating pure metal can effectively improve the interface bonding without negative effect on TC of Al matrix and harmful interfacial reaction [1, 13–16]. Li et al. [17] fabricated composite using pure W coating and uncoated diamond. The TC of the composite was increased from 494 to 564 W/mK by W coating. Zhang et al. [19] and Ren et al. [20] found that the Ti and Cr coating on the diamond could also improve the TC of the composite. Beside the kind of the coating, the thickness of the coating is critical to the TC of the composite. Yang et al. [14] prepared 35–130 nm W coatings by magnetron sputtering, and fabricated diamond/Al composites. The maximum TC of the composite was 622 W/mK, when thickness of W coating was 45 nm, whereas TC decreased to 590 W/mK as the coating thickness increased to 130 nm. Tan et al. [18] reported the similar results in the composites fabricated by diamond with 200–400 nm thick W coating.

Besides interfacial bonding, the TC of the composite can be improved by bridging the gap of the phonon velocity between diamond and Al matrix. Compared to the pure metals, the carbides have the phonon vibration modes to match diamond as well as Al matrix better [13], therefore, carbide coatings might be more effective to improve the interfacial thermal conductance (ITC). In the last few years, various carbides, such as TiC, Cr_3C_2, ZrC, B_4C and SiC [21–27], were attempted to modify the ITC. Sun et al. [26] coated 1.5 μm thick B_4C on the diamond and fabricated 50 vol.% diamond/Al composite by powder metallurgy, the composite showed a slightly improved TC of 352.7 W/mK compared to TC of 283.8 W/mK. Similar result was also found by Li et al. [27]. The diamond with 440 nm SiC coating was used to prepare 55 vol.% diamond/Al composite by vacuum pressure infiltration method. The TC of the composites was improved from 590 to 660 W/mK by SiC coating.

Similar to the metal coating on the diamond, the thickness of the carbide coating is also important to the TC of the composites. However, it is difficult to achieve thin carbide coatings on diamond due to the relative lack of nanocoating fabrication methods. Moreover, carbides and Al matrix react easily, therefore, carbide nanocoating can hardly reserve on the interface between diamond and Al matrix during manufacture. Liu et al. [16] prepared TiC nanocoating on the diamond surface to construct a diamond-TiC-Al interface, however, the desired interfacial structure could not be obtained because the nanocoating reacted off with the Al matrix. Among carbides mentioned above, WC has good thermal conduction and is relatively stable in the Al matrix [14]. However, there are few reports of the effect of WC nanocoating on the TC of diamond/Al composite. It is valuable to study the preparation process of WC nanocoatings and their effect on the interface and TC of diamond/Al composites.

In this study, nano-WC coatings were successfully fabricated on diamond surfaces by sol–gel and in situ reaction methods. The diamond/6061 Al composites were prepared by powder metallurgy method. The WC coating on the diamond surface and the interface in the composite were observed by scanning electron microscopy (SEM, Zeiss Supra 55), which was used to elucidate the effect of the WC coating thickness on the TC of the diamond/Al composite and the interfacial products.

2 Experimental

2.1 Preparation of the WC-Coated Diamond Particles

The synthetic diamond particles in the size range of 210–250 μm (HWD40 type, monocrystalline diamond particles) were used as reinforcement for the composites. As shown in Fig. 1, the surface of the diamond particles has six square

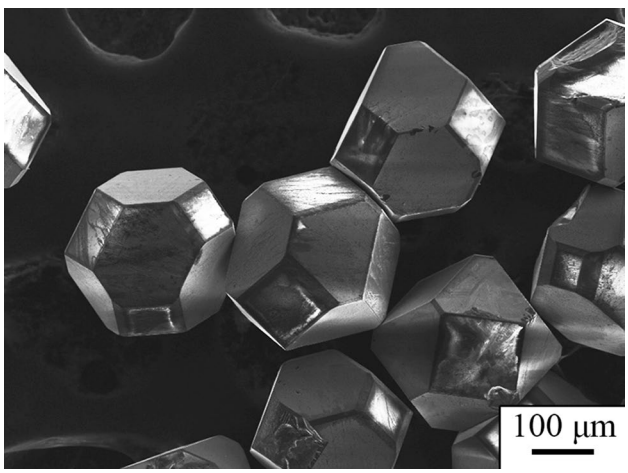

Fig. 1 Morphology of as-received diamond particles

planes ({100} planes) and eight hexagonal planes ({111} planes). Nitrogen content of the diamond was 180 ppm measured by a nitrogen/oxygen/hydrogen tester. Based on the data of Yamamoto [7], the intrinsic TC of diamond in this work was assumed to be 1611 W/mK.

The WC coating on the diamond particles was fabricated by a sol–gel method. 13 g tungsten powders was dissolved gradually into an 80 mL water solution of H_2O_2 with a 30% mass fraction at 0–5 °C. The obtained solution was filtered and mixed with 70 ml of anhydrous ethanol in the water bath at 40–45 °C for 8 h to form WO_3 sol–gel. Subsequently, the WO_3 sol–gel was stood for 24 h, and then was diluted to 0.2 mol/L and 0.5 mol/L using anhydrous ethanol for coating. The diamond particles were, respectively, immersed in the two concentrations of WO_3 sol–gel and mixed sufficiently for 15 min, and were dried at room temperature for 48 h. Diamond particles were pre-sintered at 450 °C for 60 min to form a WO_3 coating on the diamond. After that, the diamond particles were baked at 1250 °C for 120 min in a vacuum of less than 1.0×10^{-1} Pa to produce a WC coating. Prepared using 0.2 and 0.5 mol/L sol–gel, the WO_3-coated diamond, as well as the WC-coated diamond were noted as WO0.2, D0.2, and WO0.5, D0.5, respectively. Besides, the as-received diamond without coating was noted as D0.

2.2 Preparation of Composites

The diamond/Al composites with a volume fraction of 60% were prepared by a powder metallurgical method. The 6061 Al (Al–1.0 Mg–0.65Si–0.25Cu, wt%) powders with an average size of 150 μm were selected as the matrix alloy. D0, D0.2, and D0.5 diamond particles were, respectively, mixed with the 6061Al powder in a blender at 100 r/min for 6 h. The mixed powders were cold-pressed into a steel mold. Then the powder was heated up to 660 °C holding for 1 h and was immediately hot-pressed at 100 MPa. The fabricated diamond/Al composites are denoted as D0/Al, D0.2/Al, and D0.5/Al depending on the diamond particles used.

2.3 Characterizations

X-ray diffraction (XRD, D/Max-2500PC, Cu $K\alpha$ radiation) was used to examine phases of the coated diamond particles and their composites. X-ray photoelectron spectroscopy (XPS, Thermo ESCALAB250) was used to analyze chemical composition of the coatings. Surface morphologies of the diamond particles as well as interfaces of the composites were observed by SEM. The SEM samples were prepared using an ion beam milling system (Leica EM TIC 3X). The TC of the composites was calculated according to Eq. (1):

$$\lambda = \rho\alpha C, \tag{1}$$

where λ, ρ, α, and C are the thermal diffusion, density, thermal diffusivity, and heat capacity of the composites, respectively.

Thermal diffusion was measured by the laser flash method using a disk specimen 12.7 mm in diameter and 3 mm in thickness. Density of the composites was measured by the Archimedes method. Specific heat was measured by differential scanning calorimetry (DSC; NETZSCH STA 499 C, Germany) using a disk specimen 4 mm in diameter and 1 mm in thickness.

3 Results and Discussion

3.1 Microstructure of WC-Coated Diamond

Figure 2 shows the XRD patterns of the diamond particles. For the as-received diamond particles (Fig. 2a), there are only diamond peaks, indicating the absence of impurities in the diamond particles. For the WO0.2 (Fig. 2b), the peaks of WO_3 appear, which indicate the gelation of WO_3 during the pre-sintering process. For the D0.2 (Fig. 2c), in addition to the diamond peaks, there were also WC peaks, and the WO_3 peaks disappeared, indicating that the WO_3 completely reacts with the carbon on the diamond surface.

Figure 3 shows the morphologies of D0.2 and D0.5 samples. The coatings of D0.2 was nonuniform (Fig. 3a), {100} planes were completely covered by continuous and dense coating (Fig. 3b), whereas the coatings were discontinuous with droplet-shaped on the {111} planes (Fig. 3c). This result suggests that coatings were preferentially deposited on the {100} planes where the surface energy is higher. The results are similar to the report by Yang et al. [28]. Due

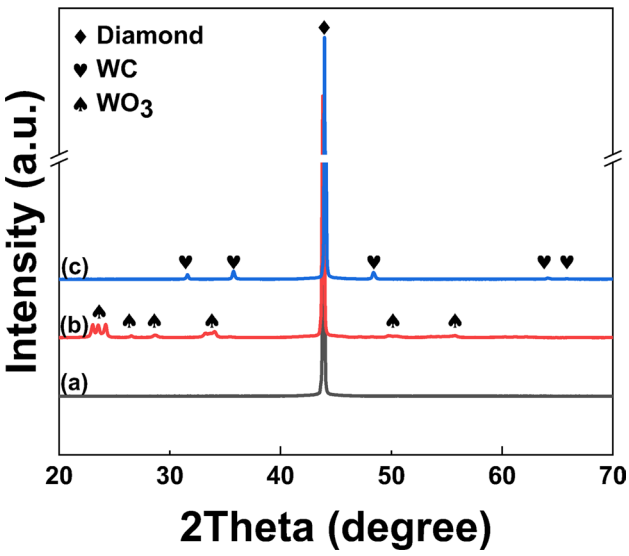

Fig. 2 X-ray diffraction patterns of **a** D0; **b** WO0.2; **c** D0.2

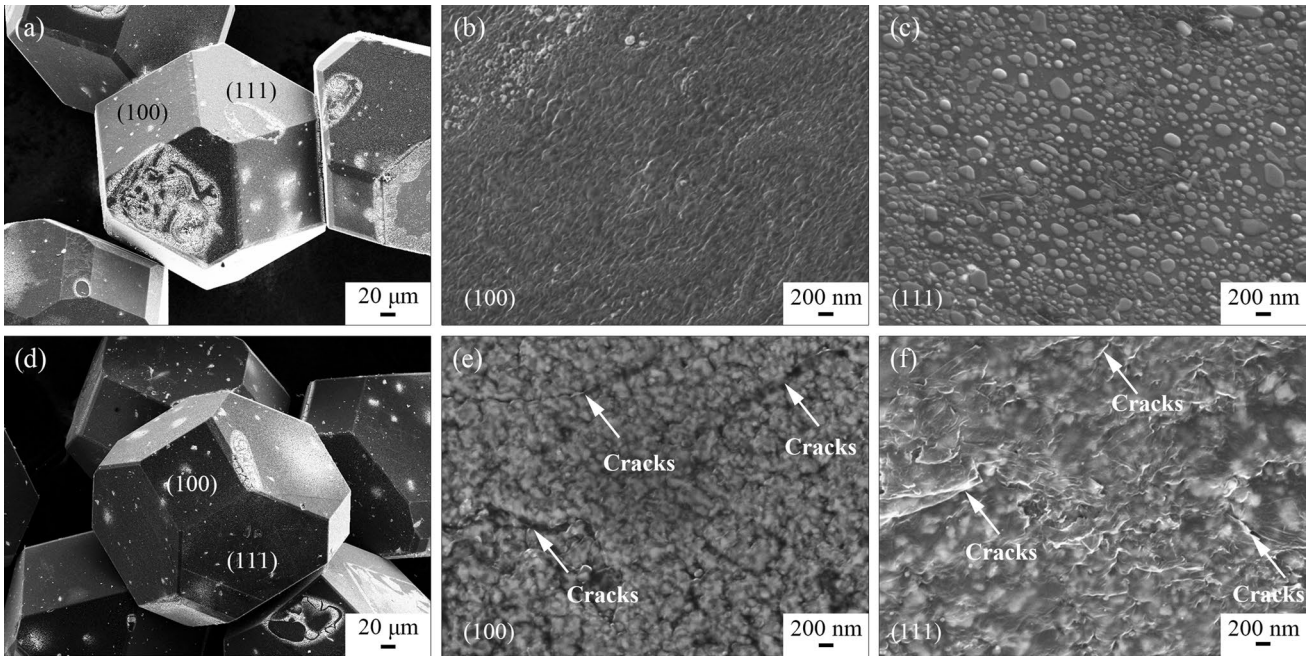

Fig. 3 SEM images of diamond particles: **a** D0.2; **b** {100} plane of D0.2; **c** {111} plane of D0.2; **d** D0.5; **e** {100} plane of D0.5; **f** {111} plane of D0.5

to the relatively lower concentration of sol–gel, the WO_3 colloidal particles in the sol–gel were not enough to fully deposited on the {111} planes of diamond particles. When the concentration of WO_3 sol–gel increased to 0.5 ml/L, the surface of the diamond was completely covered with a coating (Fig. 3d). The {100} planes of the diamond were covered with a continuous rough coating, and there is a large number of cracks on the surface of the coating (Fig. 3e). Unlike the discontinuous coatings on the {111} planes of D0.2, the {111} planes of D0.5 were covered with continuous and uniform coatings, and there existed also several cracks (Fig. 3f). The higher concentration of WO_3 sol–gel produced more WC during the sintering process. Therefore, the thickness of the WC coating would increase, which could result in the coating cracking due to thermal stress.

XPS was used to identify the elements and to estimate the surface chemistry of the coating. Figure 4a shows the survey scan of D0.2. C1*s*, O1*s*, W4*p*, W4*d*, and W4*f* are present, which shows the presence of C, W, and O on the surface of diamond particles. The W4*f* spectrum exhibits two contributions, W5/2*f* and W7/2*f* (from spin–orbit splitting) located at 34.10 eV and 32.2 eV, respectively

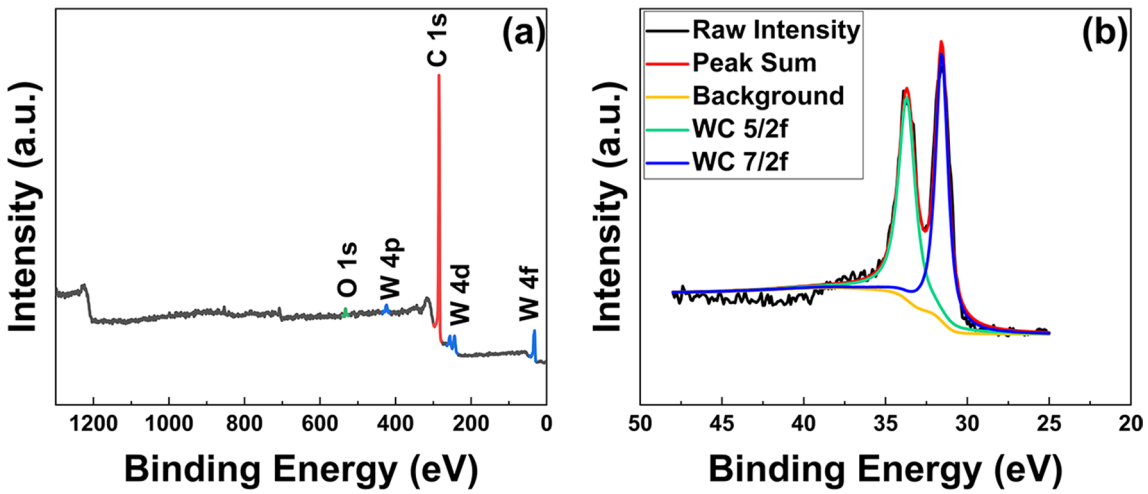

Fig. 4 XPS patterns: **a** full XPS spectrum of WC coating of D0.2; **b** high-resolution XPS spectrum of WC coating of D0.2

(Fig. 4b), both of which can be assigned to WC. Notably, the W4*f* spectrum does not exhibit contributions from W5/2*f* (33.6 eV) and W7/2 (35.7 eV) of WO_3, suggesting that WO_3 has been completely consumed during the high-temperature sintering. The O1*s* could be explained by exposure to the atmosphere after the formation of the WC coating.

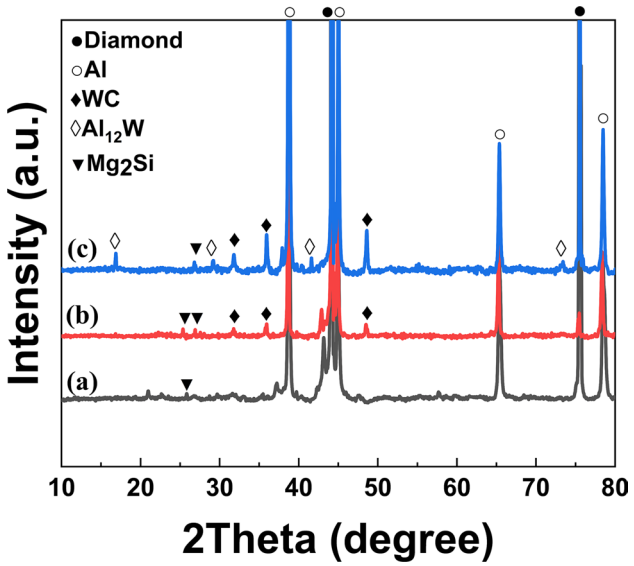

Fig. 5 XRD patterns of diamond/Al composites: **a** D0/Al; **b** D0.2/Al; **c** D0.5/Al

3.2 Microstructure of Diamond/Al Composites

Figure 5 shows the XRD patterns of the composites. The diffraction pattern for the D0/Al composite has only the peaks of the Al matrix and diamond. Different from the results of Tan et al. [15] and Zhang et al. [9], there were no peaks of the Al_4C_3 phase in the patterns of the composite. For the D0.2/Al composite, apart from the peaks of diamond and Al, the peaks of WC were presented. For the D0.5/Al composite, in addition to the peaks of diamond, Al, and WC, the peaks of $Al_{12}W$ were also identified, which suggested that the WC coating reacted with the Al matrix.

Figure 6a–c shows the SEM images of the interface in the D0/Al composite. In Fig. 6a, the black part is the diamond and the gray part is the Al matrix. The diamond and Al matrix had a well interfacial bonding on most of interface, marked by the black arrows. However, some cracks were also observed on part of interface, as marked by the white arrows, the cracks were presented both on the {100} and {111} planes of the diamond particles. Figure 6b and c shows the magnified graphs of the cracks both on the {100} and {111} planes of the diamond particles. The SEM images prove that the interfacial debonding occurred for the composite using the uncoated diamond. Figure 6d–f shows the microstructure of the D0.2/Al composite. Different to the D0/Al composite, there were no cracks on the interface between diamond and Al matrix. In Fig. 6e, a continuous and uneven interlayer with a thickness about 300 nm has been found between the {100} planes of the diamond and

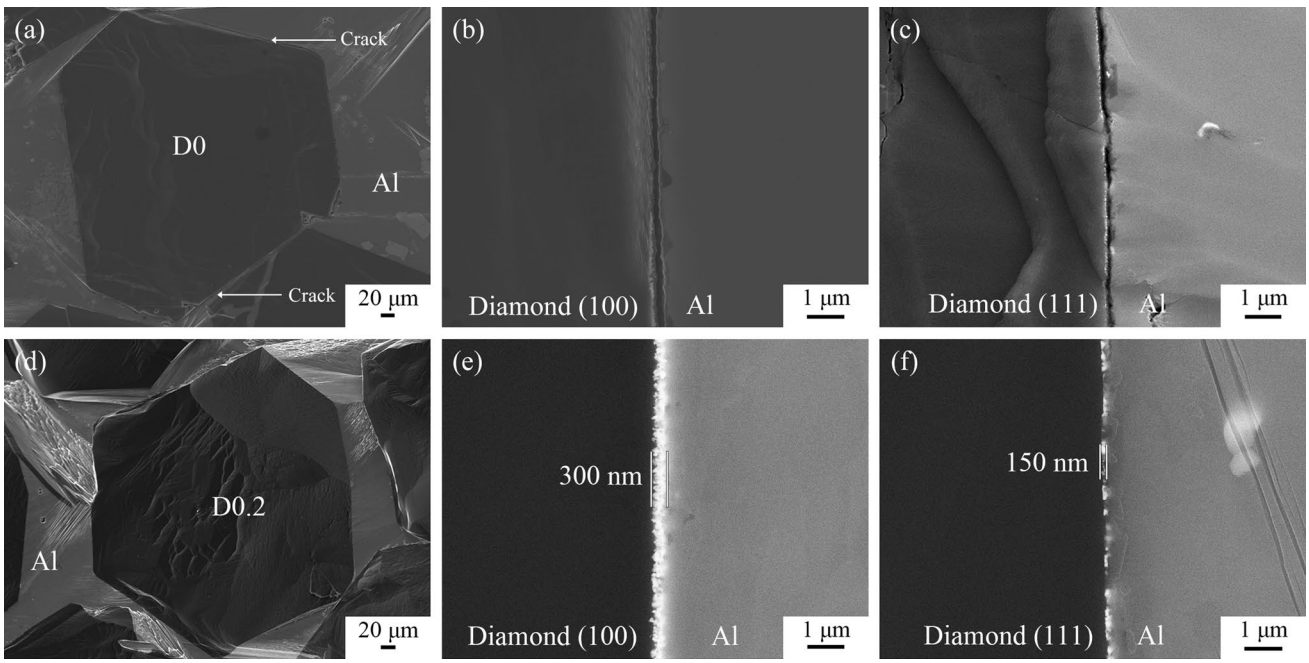

Fig. 6 Microstructures of **a**, **b**, **c** D0/Al composite; **d**, **e**, **f** D0.2/Al composite; **b**, **e** interface between diamond {100} plane and Al; **c**, **f** interface between diamond {111} plane and Al

the Al matrix. However, a non-continuous interlayer with a thickness of about 150 nm exists between the {111} planes of the diamond and the Al matrix (Fig. 6f). The variant interface results from the covering surface of WC coating, as shown by Fig. 3b and c. WC coating completely covered the {100} planes of the diamond, whereas was discontinuously covered on the {111} planes of diamond. These results indicate that in-situ WC coating was relatively stable in Al matrix and the expired interfacial structure was obtained.

Figure 7a shows SEM images of the D0.5/Al composite. Similar to the D0/Al composite, some cracks were presented on several interfaces between diamond and Al matrix, marked by the white arrows. The interfaces between diamond {100} planes and Al matrix are shown in Fig. 7b and c. There are two main different characteristics of the interface along diamond {100} planes. As shown in Fig. 7b, rough and loose WC interlayers with a thickness of 700 nm were observed. Part of the WC coating reacted with the Al matrix, thereby forming $Al_{12}W$ which was confirmed by the XRD pattern (Fig. 5c). In Fig. 7c, the WC interlayer was completely detached from the diamond. A similar phenomenon was presented on the interface between the diamond {111} plane and Al matrix, as shown in Fig. 7d. This determined that the WC coating did not distribute uniformly on the surface of the D0.5 diamond sample. Moreover, there were many cracks in the WC coating in the D0.5 diamond sample, shown in Fig. 3e and Fig. 3f, which produced by the residual stress during the fabrication process when the coating became thick. The cracks would lead to the coating peeling off during the fabrication process of the composite. Therefore, the interface bonding deteriorated and some cracks were observed on the interface between diamond and Al matrix. The coating of D0.5 diamond was not the dense, shown in Fig. 7b, due to the thickness of the layer increasing. Meanwhile, the peeled WC coating would increase the contact area between the Al matrix and the WC phases. Both of these would promote the reaction of the WC and Al matrix. Therefore, some $Al_{12}W$ phases were presented near the interface between diamond and Al matrix in the D0.5/Al composite.

3.3 Thermal Properties of Composites

The densities of the composites are tested in order to calculate TC by Eq. (1), as listed in Table 1, the density of D0/Al, D0.2/Al, and D0.5/Al is 3.127, 3.164, and 3.124 g/

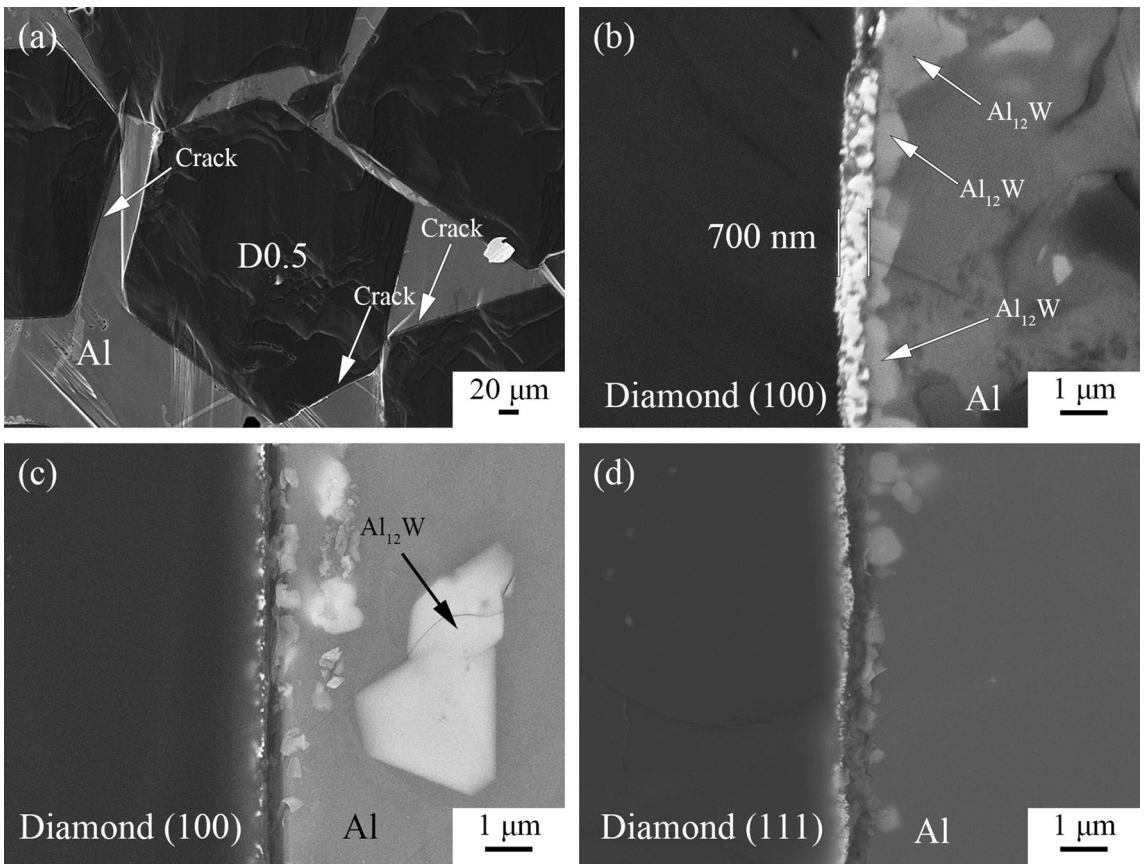

Fig. 7 Microstructures of **a** D0.5/Al composite; **b**, **c** interface between diamond {100} plane and Al; **d** interface between diamond {111} plane and Al

Table 1 Thermal properties of diamond/Al composites

	Density (g/cm^3)	Relative density (%)	Thermal conductivity (W/mK)
D0/Al	3.127	98.3	584.7
D0.2/Al	3.164	99.5	626.1
D0.5/Al	3.124	98.2	584.2

Table 2 Thermal physical parameters of different materials

Material	Density (kg/m^3)	TC (W/mK)	Specific heat capacity (J/kg K)	Phonon velocity (m/s)
Diamond	3520	1800	512	13,430
Al	2700	230	895	3620
WC	14,900	120	203	4697

cm^3, attained 98.3, 99.5 and 98.2% of the theoretical value, respectively. The relatively lower density of D0/Al composite might be attributed to the poor interfacial bonding between uncoated diamond and Al matrix, as shown in Fig. 6a–c. For the D0.2/Al composite, the interface between diamond and Al matrix was well without cracks (Fig. 6e and f). For the D0.5/Al composite, similar to the D0/Al composite, some cracks were presented on the interface due to peeling off the WC coating from the diamond. The results indicate that the density of the composite was changed with interface bonding.

Table 1 lists the TC of the composites. The D0/Al, D0.2/Al, and D0.5/Al composites have TC of 584.7, 626.1, and 584.2 W/mK, respectively. The TC of the D0.2/Al was higher than that of the composite using ZrC-coated diamond [29], in which the size of the diamond and the thickness of the ZrC coatings was similar to this work. However, the volume fraction of diamond in the composite using ZrC-coated diamond was 60%, which was higher than this work. This indicates the WC coating was benefit to improve the thermal conductivity of diamond/Al composites.

To estimate the effect of the interface on the TC of the composites, the ITC was used to eliminate distraction by the particles' size and content. The differential effective medium (DEM) model has been demonstrated to be effective for the calculation of ITC for metal matrix composite [30–32]. The diamond particles in the composites were simplified to spheres. The TC of the composite K_c can be expressed as the following expression:

$$\left(1-V_r\right)\left(\frac{K_c}{K_m}\right)^{\frac{1}{3}}=\frac{K_r^{eff}-K_c}{K_r^{eff}-K_m}, \tag{2}$$

where K is the TC, and subscript c, m, r represents the composite and matrix and diamond, respectively. K_r^{eff} is the equivalent TC of diamond particles, which can be expressed as the following equation:

$$K_r^{eff}=\frac{K_r}{1+\frac{k_r}{h_c a}}, \tag{3}$$

where a is the diameter of the reinforcement particles, h_c is the ITC of the composite.

Considering that the main thermal-carrier heat transport between diamond and Al matrix is phonon, in this study, ITC between the two phases could be estimated by the acoustic mismatch model (AMM) [33]. The ITC calculated by the AMM model is an ideal theory value, which did not consider the defect and impurity of the diamond. The ITC at the two-phase interface can be expressed as the following equation:

$$h=\frac{1}{2}\rho_l c_r \frac{v_l^3}{v_r^2}\frac{\rho_l v_l \rho_r v_r}{\left(\rho_l v_l+\rho_r v_r\right)^2}, \tag{4}$$

where v is the phonon velocity, and c is the specific heat capacity, the subscript l represents the phonon incident side and r represents the phonon scattering side.

Based on the physical parameters listed in Table 2, the ITC of various two-phase interfaces can be calculated. The ITC for the direction of heat conduction from the diamond side to the Al side is 4.5×10^7 W/m^{2}K ($h_{\text{diamond-Al}}$). The ITC for the direction of heat conduction from the diamond side to the WC side is 2.38×10^{10} W/m^{2}K ($h_{\text{diamond-WC}}$). The ITC for the direction of heat conduction from the WC side to the Al side is 1.29×10^9 W/m^{2}K ($h_{\text{WC-Al}}$).

The TC of the D0/Al composite is 584.7 W/mK. According to the DEM model, the ITC of the D0/Al composite ($h_{\text{D0/Al}}$), calculated by Eqs. (2) and (3), is 1.89×10^7 W/m^{2}K. However, calculated by the AMM model (Eq. 4), the ITC of D0/Al composite ($h_{\text{diamond-Al}}$) is 4.5×10^7 W/m^{2}K. It can be seen that there is a large difference between the actual ITC and the AMM calculated value of the D0/Al composite, which can be attributed to the weaker interfacial bonding between diamond and Al. For the D0.2/Al composite, the TC is 626.1 W/mK. The ITC calculated by the DEM model ($h_{\text{D0.2/Al}}$) is 3.2×10^7 W/m^{2}K which increased 69.3% compared to that of the D0/Al composite ($h_{\text{D0/Al}}$). The nano-WC coating could improve interfacial bonding between diamond and Al matrix and increased the density of the composite. Therefore, the ITC and TC of the composite increased significantly. The similar results were reported in the composites using the diamond coated by the TiC and ZrC [16, 29]. However, the increment of the ITC was lower than that of the diamond coated by WC.

The WC interlayer changed interface from a simple pair of diamond-Al to diamond-WC-Al. As shown in Fig. 8,

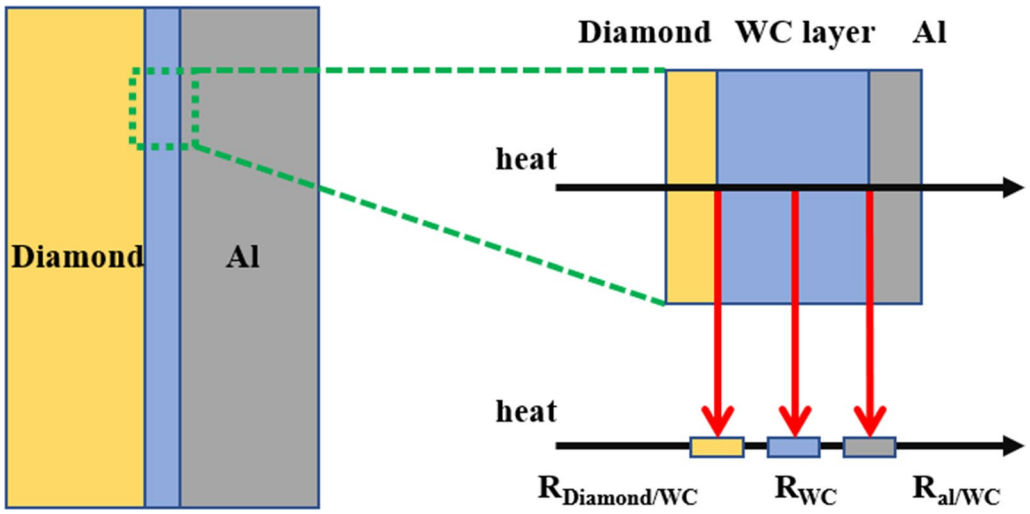

Fig. 8 Schematic diagram of diamond/Al composite interface structure

the path of phonon transmission at the interface of the D0.2/Al composite consists of the following three components: (1) the interface between diamond and WC coating; (2) the interface between Al matrix and WC coating; (3) the thermal resistance of WC coating. The total ITC can be obtained by summing up the thermal resistance of the above three parts, which can be expressed as the following equations:

$$\frac{1}{h} = R = \frac{1}{h_{\text{Diamond - WC}}} + \frac{1}{h_{\text{WC}}} + \frac{1}{h_{\text{WC - Al}}} . \tag{5}$$

$$\frac{1}{h_{\text{WC}}} = R_{\text{WC}} = \frac{l}{K_{\text{WC}}} . \tag{6}$$

where l is the thickness of the interlayer at the composite interface. The ITC and interfacial thermal resistance R are reciprocal to each other.

Assuming that the surface of D0.2 has a continuous dense WC coating with a thickness of 300 nm based on results shown by Fig. 2e. The ITC of the D0.2/Al interface calculated by Eq. (5) is 3.01×10^8 W/m^{2}K, is more than ten times of that calculated by the DEM model ($h_{\text{D0.2/Al}}$). The density of the D0.2/Al composite is only 99.5% of the theory value, which means that some micro-holes would present in the matrix. Moreover, the discontinuous WC interlayer on {111} planes and the unevenness of the WC interlayer on {100} planes of the diamond, shown in Fig. 6e and f, would increase the phonon scattering and influence the coupling between diamond and Al matrix. All of these would lead to the ITC calculated by the DEM model was lower than that by the AMM model.

For the D0.5/Al composite, the TC is 584.2 W/mK and the ITC calculated by the DEM model is 1.88×10^7 W/m^{2}K ($h_{\text{D0/Al}}$), which is lower than that of the D0.2/Al composite. Part of the WC coating peeling off and reacting with the matrix to form an Al-tungsten compound during the fabrication process would result in some cracks presented on the interface, which would decrease the ITC of the composite. As shown in Fig. 6b–d, there is some loose WC interlayers about 700 nm on the interface, which is also harmful to the ITC.

Depending on the above results, it can be considered that WC coating about 300 nm could improve the interface bonding of the composite significantly. Although some defects reduced ITC compared to the value calculated by AMM model, the 300 nm thick WC coating still could improve the ITC and TC of the composite. However, when the thickness of the WC coating increased, more defects formed on the interface due to the coating broken and peeled off from the interface. Then, some cracks were observed on the interface and the TC of the composite was similar to that of the composite fabricated by the diamond without coating. Therefore, designing a WC layer on the interface with an appropriate thickness was benefit to achieve a diamond /Al composite with high TC.

4 Conclusions

1. WC coatings were prepared on diamond particles by sol–gel and in-situ synthesis methods. The WC coating prepared by sol–gel with 0.2 mol/L can effectively enhance the bonding between diamond and Al matrix and increase the density of the composite from 98.3 to 99.5% of the theoretical density.
2. The WC interlayer with the thickness of 300 nm, could improve ITC significantly. Although the layer was discontinuous on {111} planes of the diamond, the TC of

the composite could also reach 626.1 W/mK. Moreover, the ITC could increase 69.3% compared to that of the composite using the diamond without coating.

3. Excessively thick WC coatings (thicker than 700 nm) tend to peel off during the fabrication process of composite, limiting the role of the coatings in improving interfacial bonding.

Acknowledgements This work was financially supported by the National Natural Science Foundation of China (No. 51931009) and the Liaoning Revitalization Talents Program (No. XLYC2007009).

Declarations

Conflict of interest The authors declare that they have no known competing financial interests or personal relationships that could have appeared to influence the work reported in this paper.

References

[1] A.M. Abyzov, S.V. Kidalov, F.M. Shakhov, J. Mater. Sci. **46**, 1424 (2011)
[2] K. Yoshida, H. Morigami, Microelectron. Reliab. **44**, 303 (2004)
[3] A.L. Moore, L. Shi, Mater. Today **17**, 163 (2014)
[4] J.D. Mathias, P.M. Geffroy, J.F. Silvain, Appl. Therm. Eng. **29**, 2391 (2009)
[5] T.H. Nam, G. Requena, P. Degischer, Compos. Part A Appl. Sci. Manuf. **39**, 856 (2008)
[6] C. Xue, J.K. Yu, X.M. Zhu, Mater. Des. **32**, 4225 (2011)
[7] Y. Yamamoto, T. Imai, K. Tanabe, T. Tsuno, Y. Kumazawa, N. Fujimori, Diam. Relat. Mater. **6**, 1057 (1997)
[8] L. Wei, P.K. Kuo, R.L. Thomas, T.R. Anthony, W.F. Banholzer, Phys. Rev. Lett. **70**, 3764 (1993)
[9] Y. Zhang, J.W. Li, L.L. Zhao, X.T. Wang, J. Mater. Sci. **50**, 688 (2015)
[10] W.L. Yang, K. Peng, J.J. Zhu, D.Y. Li, L.P. Zhou, Diam. Relat. Mater. **46**, 35 (2014)
[11] C.Y. Guo, X.B. He, S.B. Ren, X.H. Qu, J. Alloy. Compd. **664**, 777 (2016)
[12] C. Edtmaier, J. Segl, E. Rosenberg, G. Liedl, R. Pospichal, A. Steiger-Thirsfeld, J. Mater. Sci. **53**, 15514 (2018)
[13] C. Azina, I. Cornu, J.F. Silvain, Y.F. Lu, J.L. Battaglia, AIP Adv. **9**, 055315 (2019)
[14] W.S. Yang, G.Q. Chen, P.P. Wan, J. Qiao, F.J. Hu, S.F. Liu, Q. Zhang, M. Hussain, R.H. Dong, G.H. Wu, J. Alloy. Compd. **726**, 623 (2017)
[15] Z.Q. Tan, G. Ji, A. Addad, Z.Q. Li, J.F. Silvain, D. Zhang, Compos. Part A Appl. Sci. Manuf. **91**, 9 (2016)
[16] X.Y. Liu, W.G. Wang, D. Wang, D.R. Ni, L.Q. Chen, Z.Y. Ma, Mater. Chem. Phys. **182**, 256 (2016)
[17] G. Ji, Z.Q. Tan, Y.G. Lu, D. Schryvers, Z.Q. Li, D. Zhang, Mater. Charact. **112**, 129 (2016)
[18] Z. Tan, Z. Li, G. Fan, Q. Guo, X. Kai, G. Ji, L. Zhang, D. Zhang, Mater. Des. **47**, 160 (2013)
[19] Y. Zhang, H.L. Zhang, J.H. Wu, X.T. Wang, Scr. Mater. **65**, 1097 (2011)
[20] S. Ren, X. Shen, C. Guo, N. Liu, J. Zang, X. He, X. Qu, Compos. Sci. Technol. **71**, 1550 (2011)
[21] L. Wang, J. Li, M. Catalano, G. Bai, N. Li, J. Dai, X. Wang, H. Zhang, J. Wang, M.J. Kim, Compos. Part A Appl. Sci. Manuf. **113**, 76 (2018)
[22] G. Chang, F.Y. Sun, J.L. Duan, Z.F. Che, X.T. Wang, J.G. Wang, M.J. Kim, H.L. Zhang, Acta Mater. **160**, 235 (2018)
[23] C. Xue, J.K. Yu, Emerg. Mater. Res. **1**, 99 (2012)
[24] L.H. Wang, J.W. Li, Z.F. Che, X.T. Wang, H.L. Zhang, J.G. Wang, M.J. Kim, J. Alloys Compd. **749**, 1098 (2018)
[25] Y. Pan, X. He, S. Ren, M. Wu, X. Qu, Materials **12**, 475 (2019)
[26] Y.H. Sun, C. Zhang, L.K. He, Q.N. Meng, B.C. Liu, K. Gao, J.H. Wu, Sci. Rep. **8**, 1 (2018)
[27] X. Li, W. Yang, J. Sang, J. Zhu, L. Fu, D. Li, L. Zhou, J. Alloy. Compd. **846**, 156258 (2020)
[28] W.L. Yang, J.Q. Sang, L.P. Zhou, K. Peng, J.J. Zhu, D.Y. Li, Diam. Relat. Mater. **81**, 127 (2018)
[29] N. Li, L. Wang, J. Dai, X. Wang, J. Wang, M.J. Kim, H. Zhang, Diam. Relat. Mater. **100**, 107565 (2019)
[30] D.P.H. Hasselman, L.F. Johnson, J. Compos. Mater. **21**, 508 (1987)
[31] V. Sinha, J.E. Spowart, J. Mater. Sci. **48**, 1330 (2013)
[32] L.H. Wang, J.W. Li, G.Z. Bai, N. Li, X.T. Wang, H.L. Zhang, J.G. Wang, M.J. Kim, J. Alloy. Compd. **781**, 800 (2019)
[33] M.Y. Yuan, Z.Q. Tan, G.L. Fan, D.B. Xiong, Q. Guo, C.P. Guo, Z.Q. Li, D. Zhang, Diam. Relat. Mater. **81**, 38 (2018)